Cell

Increased Ethanol Resistance and Consumption in *Eps8* Knockout Mice Correlates with Altered Actin Dynamics

Nina Offenhäuser,[1,9,*] Daniela Castelletti,[1,9] Lisa Mapelli,[2] Blanche Ekalle Soppo,[1] Maria Cristina Regondi,[3] Paola Rossi,[2] Egidio D'Angelo,[2] Carolina Frassoni,[3] Alida Amadeo,[4] Arianna Tocchetti,[1] Benedetta Pozzi,[1] Andrea Disanza,[1,5] Douglas Guarnieri,[6] Christer Betsholtz,[7] Giorgio Scita,[1,5] Ulrike Heberlein,[6] and Pier Paolo Di Fiore[1,5,8,*]

[1] Fondazione Istituto FIRC di Oncologia Molecolare, Via Adamello 16, 20139 Milan, Italy
[2] Dipartimento di Scienze Fisiologiche e Farmacologiche Cellulari e Molecolari, Università di Pavia, 27100 Pavia, Italy
[3] Dipartimento di Epilettologia clinica e Neurofisiologia Sperimentale, Istituto Nazionale Neurologico C. Besta, 20133 Milan, Italy
[4] Dipartimento di Scienze Biomolecolari e Biotecnologie, Università degli Studi di Milano, 20133 Milan, Italy
[5] Dipartimento di Oncologia Sperimentale, Istituto Europeo di Oncologia, 20141 Milan, Italy
[6] Department of Anatomy and Program in Neuroscience, University of California, San Francisco, San Francisco, CA 94143, USA
[7] Department of Medical Biochemistry and Biophysics, Karolinska Institutet, 171 77 Stockholm, Sweden
[8] Dipartimento di Medicina, Chirurgia ed Odontoiatria, Università degli Studi di Milano, 20122 Milan, Italy
[9] These authors contributed equally to this work.
*Contact: nina.offenhauser@ifom-ieo-campus.it (N.O.), pierpaolo.difiore@ifom-ieo-campus.it (P.P.D.F.)
DOI 10.1016/j.cell.2006.09.011

SUMMARY

Dynamic modulation of the actin cytoskeleton is critical for synaptic plasticity, abnormalities of which are thought to contribute to mental illness and addiction. Here we report that mice lacking Eps8, a regulator of actin dynamics, are resistant to some acute intoxicating effects of ethanol and show increased ethanol consumption. In the brain, the N-methyl-D-aspartate (NMDA) receptor is a major target of ethanol. We show that Eps8 is localized to postsynaptic structures and is part of the NMDA receptor complex. Moreover, in Eps8 null mice, NMDA receptor currents and their sensitivity to inhibition by ethanol are abnormal. In addition, Eps8 null neurons are resistant to the actin-remodeling activities of NMDA and ethanol. We propose that proper regulation of the actin cytoskeleton is a key determinant of cellular and behavioral responses to ethanol.

INTRODUCTION

Alcoholism affects approximately 300 million people worldwide. Resistance to the acute intoxicating effects of ethanol is a risk factor for the development of alcoholism and is genetically determined, at least in part (Schuckit and Smith, 2000). Thus, the understanding of the molecular mechanisms underlying ethanol resistance might provide important clues about alcohol addiction.

One of the most sensitive targets of ethanol in the brain is the excitatory N-methyl-D-aspartate (NMDA) receptor (NMDAR), whose activity is inhibited by ethanol (Hoffman et al., 1989; Lovinger et al., 1989). Additionally, many of the adaptive responses to ethanol in the brain are ascribed to compensatory changes in NMDAR activity (Carpenter-Hyland et al., 2004; Roberto et al., 2004; Ron, 2004; Woodward, 2000). The NMDAR is localized in dendritic spines of central neurons, where it is part of a multimolecular complex (NMDAR complex) comprising nearly a hundred proteins involved in the scaffolding, regulation, and signal transduction of the receptor (Husi et al., 2000). Activity-dependent changes in the composition of the complex are important in the regulation of the NMDAR and are part of the biochemical and structural changes involved in synaptic plasticity (Sheng and Kim, 2002). The NMDAR complex is attached to the actin cytoskeleton (Wyszynski et al., 1997), which is also dynamically remodeled in response to synaptic activity (Dillon and Goda, 2005). Whether actin dynamics and associated regulation of the NMDAR complex play a role in ethanol-related behavior is still an open question.

The Eps8 family of proteins comprises four members: Eps8, Eps8L1, Eps8L2, and Eps8L3 (Offenhäuser et al., 2004). The best characterized member of the family, Eps8, is involved in the regulation of actin dynamics via at least two different mechanisms. On the one hand, Eps8 contributes to the activation of Rac by growth-factor receptors (Innocenti et al., 2002, 2003; Scita et al., 1999); on the other, it is endowed with actin barbed-end-capping activity (Croce et al., 2004; Disanza et al., 2004). In the nematode *C. elegans*, where only one Eps8 family member is present, its deletion causes dramatic phenotypes and lethality, indicating an important role in organismal

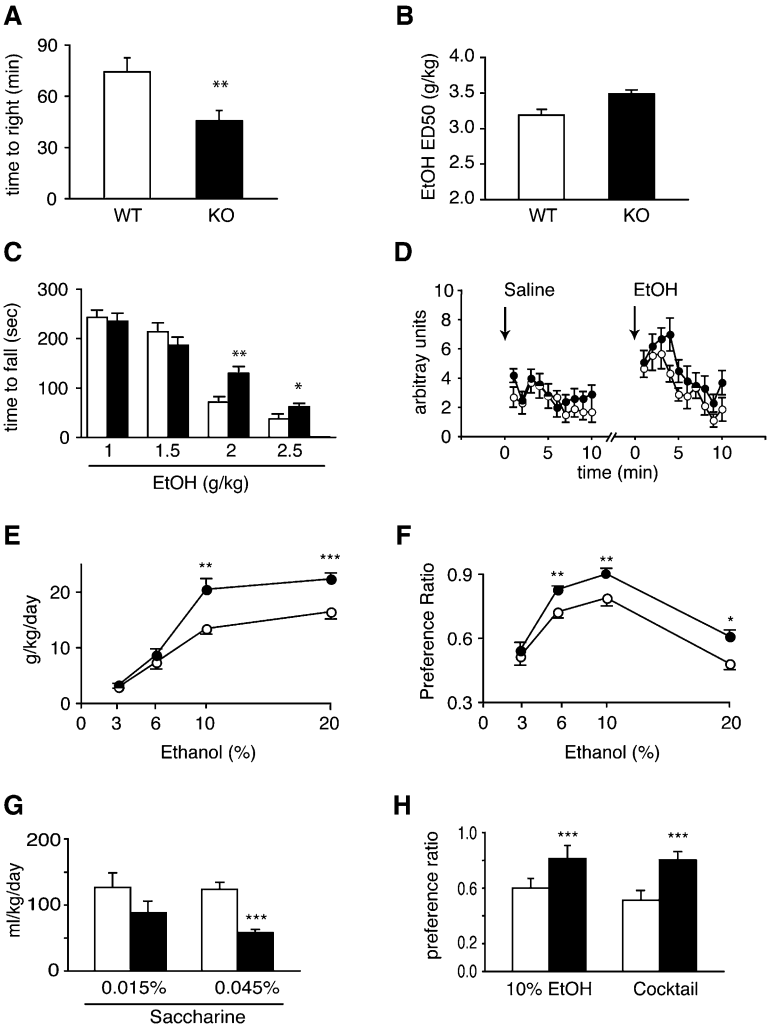

Figure 1. Ethanol-Related Phenotypes in *Eps8*-KO Mice

In this and all subsequent figures, data are expressed as average values ± SEM (standard error of the mean) unless otherwise indicated. *p < 0.05, * *p < 0.01, * * *p < 0.005.

(A) Wild-type (WT) or *Eps8*-KO (KO) mice (n = 14/group) were injected i.p. with ethanol (4 g/kg), and the righting reflex was measured.

(B) Ethanol ED_{50} for loss of righting reflex in WT and KO female mice (n = 6/group). Data, expressed as mean values ± 95% Ci, were significantly different between genotypes.

(C) WT (white bars) or KO (black bars) mice (n = 10/group) were tested on the accelerated rotarod after i.p injection of the indicated concentrations of ethanol.

(D) WT (white circles) or KO (black circles) mice (n = 10/group) were tested for locomotor activity in the open field after i.p. injection of saline or 1.5 g/kg ethanol.

(E and F) WT (white circles) or KO (black circles) littermate mice (n = 16) were tested using the two-bottle choice paradigm at the indicated concentrations of ethanol. Data are expressed as ethanol consumption (g/kg/day) (E) or as ethanol preference ratio, i.e., ethanol consumption per total fluid consumption (F).

(G) WT (white bars) or KO (black bars) mice (n = 8) were tested for consumption of sweet-tasting solutions using the two-bottle choice paradigm. Data are expressed as fluid consumption (ml/kg/day).

(H) Naive WT (white bars) or KO (black bars) mice (n = 8/group) were tested for ethanol preference (10% EtOH, as described in [E and F]). After one month of abstinence, the same mice were tested again for 4 days for cocktail consumption (cocktail, 10% ethanol in 0.045% saccharine).

homeostasis (Croce et al., 2004). Conversely, mice carrying a genetic deletion for *Eps8* (*Eps8*-KO mice) are healthy and fertile, with no overt phenotype (Scita et al., 1999). This is likely due to functional redundancy with other members of the family. Indeed, Eps8L1 and Eps8L2 share all known biochemical features of Eps8 and are coexpressed with Eps8 in all tissues, with the notable exception of the central nervous system (CNS) (Offenhäuser et al., 2004).

These observations led us to evaluate the role of Eps8 in behavior. Here we report that Eps8 regulates acute ethanol sensitivity and ethanol consumption in mice, and we provide evidence for mechanisms linking actin dynamics to behavioral responses to ethanol.

RESULTS

Eps8 Knockout Mice Are Less Sensitive to the Hypnotic and Motor-Incoordinating Effects of Ethanol

We investigated the effects of the loss of Eps8 on the development and function of the CNS. *Eps8*-KO mice did not show detectable abnormalities in brain architecture (data not shown). Thus, we assessed the basic behavioral and neurological profile of *Eps8*-KO mice using a modified SHIRPA protocol (Irwin, 1968). No differences with respect to wild-type mice were recorded (see Table S1 in the Supplemental Data available with this article online). However, in a secondary screen, we discovered that *Eps8*-KO mice show decreased sensitivity to the hypnotic (sedative) effects of ethanol. After ethanol administration, *Eps8*-KO mice regained their righting reflex significantly faster than their wild-type littermates (Figure 1A). In addition, significantly higher doses of ethanol were needed to induce the loss of righting reflex in *Eps8*-KO mice (Figure 1B).

We next tested sensitivity to the motor-incoordinating effects of ethanol using the accelerated rotarod (Rustay et al., 2003). *Eps8*-KO mice showed a normal learning curve (Figure S1A), demonstrating that motor learning was not impaired. However, when challenged with increasing concentrations of ethanol, *Eps8*-KO mice remained on the rotarod significantly longer than wild-type mice (Figure 1C), demonstrating that motor coordination

is less affected by ethanol in *Eps8*-KO compared to wild-type mice.

Sensitivity to ethanol is heterogeneous across tasks (Crabbe et al., 2005). Thus, we also tested whether low concentrations of ethanol, known to stimulate locomotor activity in the open field, would differentially affect *Eps8*-KO mice. Ethanol administration induced a significant increase in locomotor activity in both wild-type and *Eps8*-KO mice (Figure 1D). Two-way analysis of variance (ANOVA) showed an effect of ethanol treatment versus saline in both wild-type mice ($F_{1,90} = 15.46$, $p < 0.001$ for treatment; $F_{9,90} = 0.48$, $p < 0.888$ for time; and $F_{9,90} = 2.99$, $p < 0.0037$ for the interaction between the factors) and *Eps8*-KO mice ($F_{1,90} = 24.24$, $p < 0.0001$ for treatment; $F_{9,90} = 4.09$, $p < 0.002$ for time; and $F_{9,90} = 1.87$, $p < 0.0665$ for the interaction between the factors). Interestingly, we did not observe resistance to the locomotor-stimulatory effect of 1.5 g/kg ethanol in *Eps8*-KO mice. On the contrary, two-way ANOVA showed that locomotor activity was slightly more enhanced by ethanol in *Eps8*-KO with respect to wild-type mice ($F_{1,180} = 6.56$, $p = 0.0113$ for genotype; $F_{9,180} = 1.75$, $p = 0.08$ for time; and $F_{9,180} = 3.40$, $p = 0.0007$ for the interaction between the factors) (Figure 1D). Thus, *Eps8*-KO mice are resistant to some, but not all, of the acute effects of ethanol.

Plasma ethanol concentrations were not appreciably different between wild-type and *Eps8*-KO mice after acute administration of ethanol (Figures S1B and S1C), indicating that altered ethanol clearance and/or metabolism are not the underlying causes of the reduced ethanol sensitivity of *Eps8*-KO mice.

Eps8 Knockout Mice Show Increased Voluntary Ethanol Consumption

Studies of inbred or genetically modified mice have shown a positive correlation between resistance to the acute intoxicating effects of ethanol and preference for this drug (Bowers, 2000; Li et al., 1993). Thus, we tested *Eps8*-KO mice for ethanol consumption using the two-bottle choice paradigm (Belknap et al., 1993). *Eps8*-KO mice displayed both increased consumption and preference (Figures 1E and 1F). Two-way ANOVA showed an effect of ethanol concentration ($F_{3,18} = 88.4$, $p < 0.0001$) and genotype ($F_{1,118} = 20.21$, $p < 0.0001$) and an interaction between these factors ($F_{3,118} = 4.11$, $p = 0.0082$) for ethanol consumption. For the preference ratio, we found a highly significant effect of ethanol concentration ($F_{3,116} = 37.5$, $p < 0.0001$) and genotype ($F_{1,116} = 15.24$, $p = 0.002$), but no interaction between these factors ($F_{3,116} = 1.02$, $p = 0.3853$).

Differential taste reactivity might influence ethanol consumption (Crabbe et al., 1996). We therefore tested *Eps8*-KO mice for consumption of sweet, bitter, salty, sour, and umami solutions (Bachmanov et al., 1996). Mutant mice displayed a reduced consumption of sweet solutions containing either high-caloric sucrose (Figure S2A) or noncaloric saccharine (Figure 1G). No significant change was observed in the consumption of other tastants (Figures S2B–S2E), indicating that ablation of *Eps8* does not lead to a general impairment in taste perception. An association between sweet preference and ethanol consumption has been reported (Kampov-Polevoy et al., 1999), possibly due to the sweet taste of ethanol-containing solutions. Thus, the negative correlation observed in *Eps8*-KO mice was unexpected. Nevertheless, to formally exclude the possibility that altered taste accounted for increased ethanol preference, mice were tested for the consumption of a 10% ethanol solution containing saccharine as a sweetener. *Eps8*-KO mice still displayed a significantly increased preference for ethanol (Figure 1H), demonstrating that altered sweet perception does not account for the increased ethanol consumption. Finally, *Eps8*-KO mice did not show altered consumption of nicotine-containing solutions (Figure S2F), indicating that lack of Eps8 does not have a general impact on addictive behavior.

Eps8 Is Expressed in a Subset of Brain Areas Implicated in Ethanol Tolerance

Several brain areas have been implicated in ethanol-related behavior, including the mesolimbic reward circuit, hypothalamus, cortex, hippocampus, and cerebellum. To gain insight into which areas of the CNS are involved in Eps8 function in ethanol-related behavior, the expression of Eps8 in adult mouse brain was determined. Eps8 was expressed in several brain areas at low/moderate levels (data not shown). High levels of expression were confined to a few scattered neurons in layers II and III of the cerebral cortex (Figure 2A) and in the hippocampus (Figure 2B), two areas classically implicated in higher cognitive functions. In addition, Eps8 was highly expressed in scattered neurons in the prefrontal cortex and amygdala (Figure 2C) but was below detectability in brain areas involved in the mesolimbic reward circuit, such as the nucleus accumbens, ventral tegmental area, and bed nucleus stria terminalis. Thus, Eps8 either is not appreciably expressed or is expressed at low levels in brain areas implicated in the motivational reward leading to increased ethanol consumption. Conversely, Eps8 expression was particularly elevated in the cerebellar granule neuron (CGN) and molecular layers (Figure 2D), suggesting that the resistance of *Eps8*-KO mice to the motor-incoordinating effects of ethanol might be related to the function of Eps8 in the cerebellum.

Eps8 Is Localized in Postsynaptic Structures in Cerebellar Granule Neurons In Vivo and Is Part of the NMDAR Complex

The above results prompted us to focus on the cerebellum. In sections of the granule cell layer, we detected abundant expression of Eps8 in cerebellar glomeruli, with a pattern of expression coinciding with that of F-actin (Figure 3A), which in cerebellar glomeruli is known to be concentrated in the postsynaptic granule cell articulations (Capani et al., 2001). By immunoelectron microscopy, Eps8 was localized postsynaptically in the dendritic articulations of CGNs (Figure 3B), while it was absent from presynaptic mossy fibers. Biochemical fractionation of adult

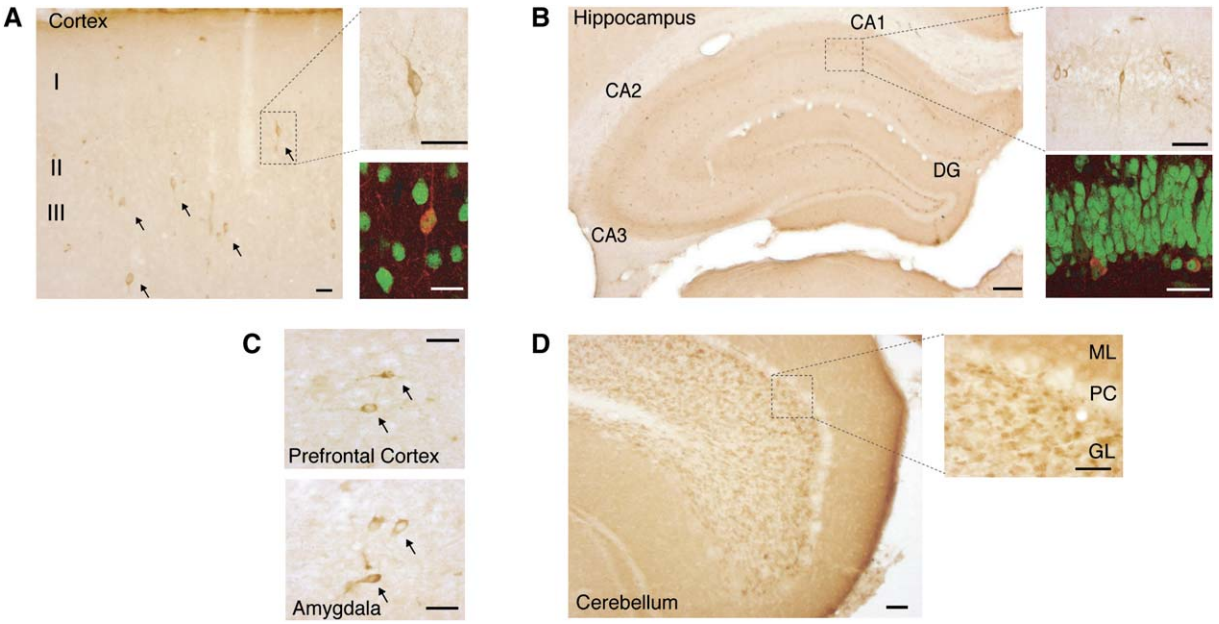

Figure 2. Localization of Eps8 in Mouse Brain

In all panels, Eps8 was detected by immunoperoxidase unless otherwise indicated.

(A) Cortex. Eps8 is expressed at high levels in a few scattered cells (arrows). Bar = 50 μm. In (A) and (B), morphology (insets) and double labeling (at bottom right) with the neuronal marker NeuN confirmed that immunoperoxidase-positive cells were neurons (Eps8 red, NeuN green). Bar = 50 μm.

(B) Hippocampus. Eps8 is expressed at high levels in scattered cells of CA1–CA3 and in the dentate gyrus (DG). Bar = 500 μm.

(C) Prefrontal cortex (top) and amygdala (bottom). Eps8 is detected in scattered neurons (arrows). Bar = 50 μm.

(D) Cerebellum. Eps8 is abundantly and uniformly expressed in the granule cell layer (GL) and the molecular layer (ML). In the granule cell layer, Eps8 is mainly localized to glomeruli (see inset), whereas the Purkinje cell layer (PC) is devoid of Eps8. Bar = 100 μm.

cerebellum further indicated that Eps8 was present in both the synaptosomal and postsynaptic density fractions (Figure 3C), consistent with the observation that Eps8 is localized both presynaptically in the molecular layer and postsynaptically in the glomeruli of the granule cell layer (Figure 2D).

The presence of Eps8 in the postsynaptic density fraction prompted us to investigate whether Eps8 and NMDAR are physically associated in vivo. In the adult cerebellum, three NMDAR subunits are expressed (Yamada et al., 2001); in Eps8 immunoprecipitates from adult cerebellum of wild-type mice (but not *Eps8*-KO mice), all three NMDAR subunits could be readily recovered (Figure 3D). This interaction was specific in that no coimmunoprecipitation between Eps8 and GluR1, a subunit of the AMPA receptor also present in the postsynaptic density fraction, was detected (Figure 3D). Similarly, Eps8—and the other two NMDAR subunits, NR2C and NR1—could be recovered in NR2A immunoprecipitates, but not in GluR1 immunoprecipitates (Figure 3E). Thus, Eps8 is part of the NMDAR complex, where it interacts, directly or indirectly, with the NMDAR.

Given the functional redundancy in the Eps8 family, it was important to establish whether Eps8 is the only member expressed in CGNs. *Eps8* mRNA was readily detected by quantitative PCR in CGNs obtained by laser capture from adult cerebellum (Figure 3F). In contrast, there was no detectable expression of *Eps8L2* and *Eps8L3* and only trace amounts of *Eps8L1* mRNA (Figure 3F). Collectively, these data indicate that Eps8 is enriched in postsynaptic structures in CGNs, where it is part of the NMDAR complex. In addition, the lack (or very low expression) of redundant members of the Eps8 family in CGNs makes these cells a good model system in which to analyze the effects of Eps8 on cellular processes related to ethanol responses.

Increased NMDA Currents and Elevated NMDAR Activity after Ethanol Exposure in *Eps8*-KO Granule Neurons

Based on the above results, and in order to understand the impact of *Eps8* ablation on CGN responses to ethanol, we measured excitatory synaptic transmission by whole-cell patch-clamp recordings from CGNs in acute cerebellar slices. Voltage-clamp recordings showed identical passive properties (membrane capacitance and input resistance) in wild-type and *Eps8*-KO CGNs (Table S2), indicating that basal parameters were not altered. Next, we recorded composite excitatory postsynaptic currents (cEPSCs) after low-frequency mossy-fiber stimulation (0.1 Hz) in the presence of bicuculline, an antagonist of inhibitory GABA receptors. To isolate the non-NMDA (−60 mV) and NMDA (+60 mV) components, two different holding potentials were used. The non-NMDA cEPSC

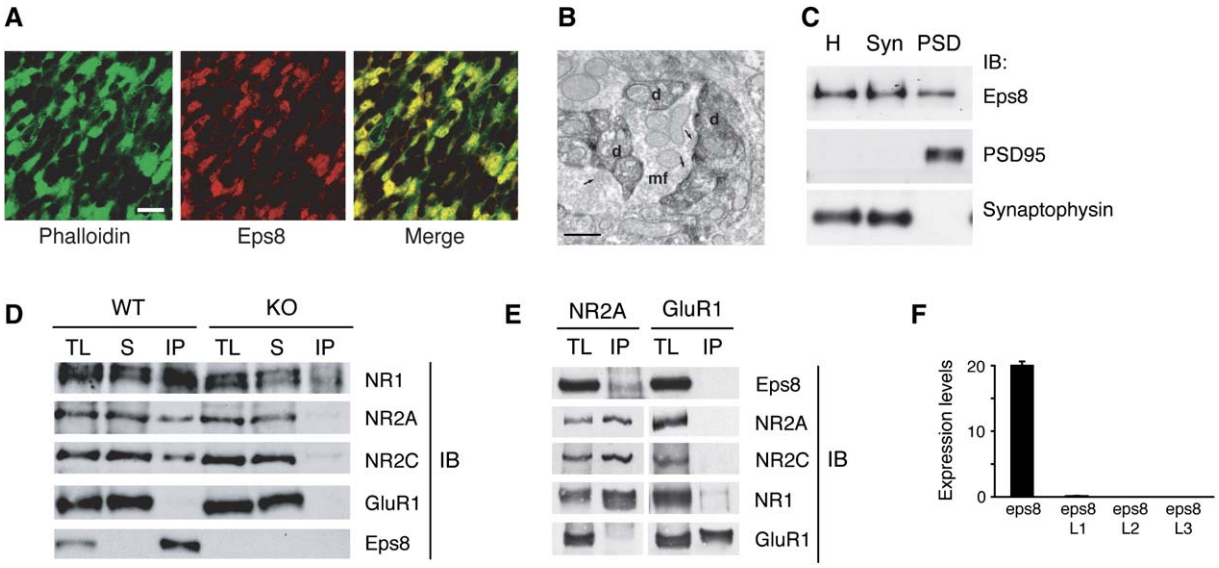

Figure 3. Eps8 and the NMDAR Complex

(A) Localization of Eps8 (red) and F-actin (phalloidin, green) in the cerebellum. Bar = 25 μm.

(B) EM analysis after pre-embedding and anti-Eps8 immunoperoxidase staining of rat cerebellar section. Eps8 staining is mostly in dendritic articulations (d) surrounding presynaptic mossy fibers (mf). Arrows point to presynaptic contact sides. Bar = 500 nm.

(C) Total cerebellar homogenate (H), the synaptosomal fraction (Syn; synaptophysin$^+$, PSD95$^-$), and the PSD fraction (SYN$^-$, PSD95$^+$) were analyzed by immunoblotting (IB) as indicated.

(D and E) Cerebellar extracts (4 mg) from WT or KO mice were immunoprecipitated with anti-Eps8 ([D], IP lanes) or with anti-NR2A or anti-GluR1 ([E], IP lanes) and immunoblotted as indicated. Aliquots (1/75) of the total lysate (TL) and the supernatant after the IP (S) were also loaded. The immunoblot in (E) was cut after probing with anti-Eps8 to allow immunoblotting with anti-NR2A (left panel) and anti-GluR1 (right panel) to check for efficient IP. The other antigens were subsequently detected after stripping of the blots.

(F) Levels of mRNA (normalized to *GAPDH*) of *Eps8* family members in laser-captured CGNs from adult cerebellum.

component showed similar amplitude and rising and decay kinetics in wild-type and *Eps8*-KO CGNs (Figures 4A–4C; Tables S3 and S4). In contrast, the NMDA cEPSC component was ~2-fold higher in *Eps8*-KO CGNs due to increased current amplitude and slower decay kinetics (Figures 4D–4F; Table S4).

To exclude the possibility that altered NMDA currents were due to alterations in neurotransmitter release we (1) recorded miniature EPSCs (minis; Figure 4A, inset), which reflect spontaneous release of neurotransmitter quanta, and (2) compared EPSC coefficient of variation (CV = SD/mean), which is altered by changes in release probability. Neither minis nor EPSC parameters were changed in *Eps8*-KO CGNs (Table S5), indicating that neurotransmitter release is normal in the cerebellum of *Eps8*-KO mice.

Finally, we tested the effect of ethanol perfusion on cEPSCs. One hundred micromolar ethanol inhibited both non-NMDA and NMDA currents in wild-type and *Eps8*-KO CGNs to a similar extent (Figures 4G and 4H). Ethanol perfusion at 400 mM did not result in further significant inhibition of non-NMDA currents. Instead, 400 mM ethanol increased the reduction of the NMDA current in wild-type neurons (from 41% to 92%, in the presence of 100 mM and 400 mM ethanol, respectively). In *Eps8*-KO CGNs, conversely, there was no additional reduction of NMDA current (~40% reduction in either 100 mM or 400 mM ethanol, Figures 4G and 4H). Inhibition of NMDA currents by ethanol was immediate and without apparent recovery during the time frame measured (Figure 4I). Finally, analysis of EPSC CV after ethanol perfusion showed no difference with respect to basal conditions in either genotype, indicating that altered presynaptic release is not responsible for the ethanol effect (Table S6).

In *Eps8*-KO CGNs, after the initial reduction of NMDA current elicited by 100 mM ethanol, there was no further reduction at higher concentrations. This suggests the existence of two components in the ethanol-induced reduction of NMDA current: an immediate one, apparently largely Eps8 insensitive, and a gradual one, which relies on the presence of Eps8. While further studies will be needed to verify this possibility, it is worth noting that the immediate component might be connected, in principle, to the reported ability of ethanol to bind and inhibit the NMDAR (Honse et al., 2004; Peoples and Stewart, 2000). The gradual Eps8-dependent component is most likely linked, as will subsequently become clear, to actin stability. (We note that this does not imply that the hypothesized immediate component is not linked to actin dynamics.) Whatever the case, given the higher charge transfer through the NMDAR in *Eps8*-KO neurons under basal conditions, application of either 100 or 400 mM ethanol

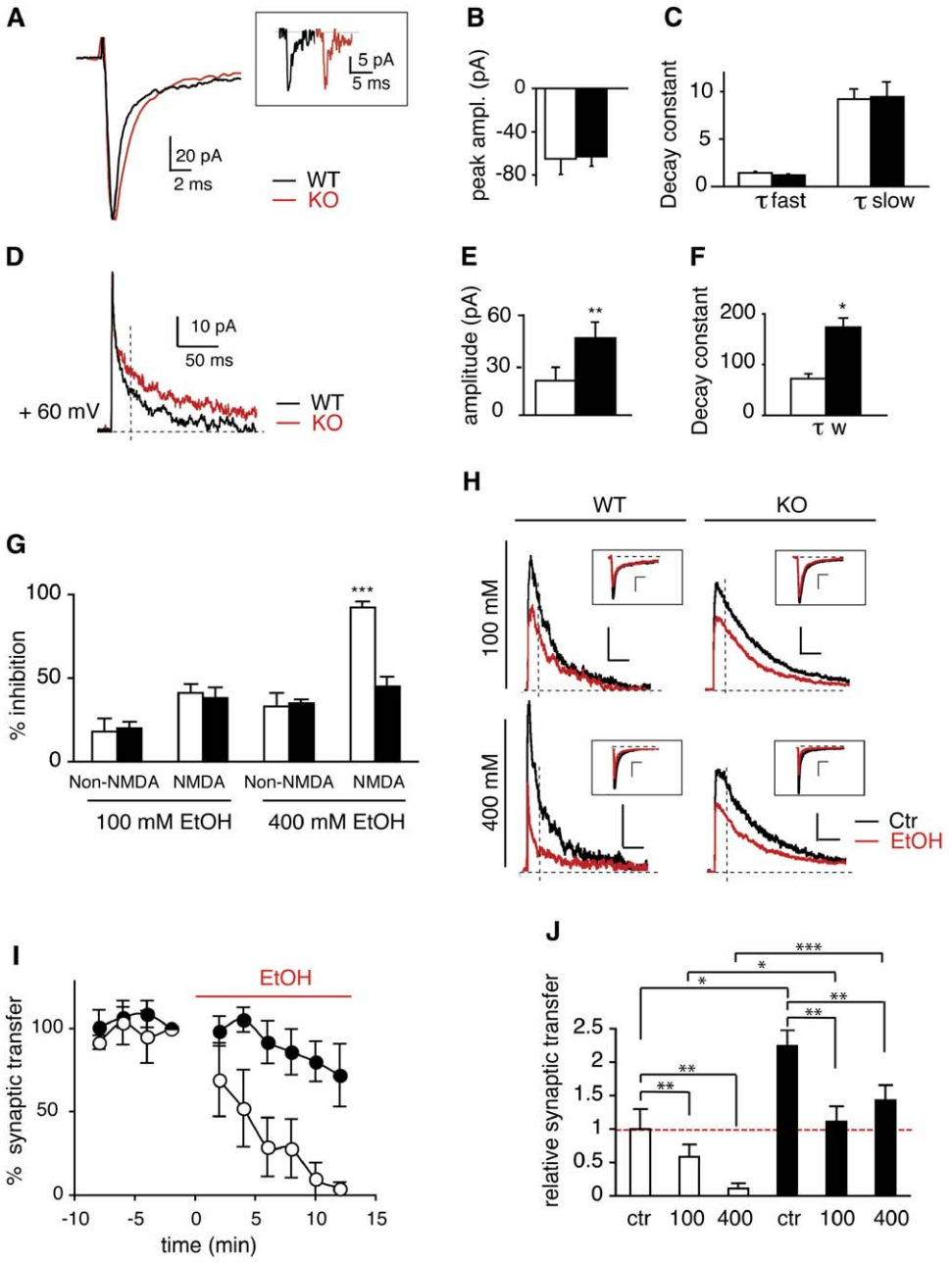

Figure 4. NMDA Currents in *Eps8*-KO Mice

(A) Superimposed average non-NMDA components in cEPSCs of WT (black) and KO (red) neurons (from acute cerebellar slices, in this and all other electrophysiological experiments) normalized for WT peak amplitude. Currents were recorded at −60 mV of holding potential. The inset shows mini recordings. Minis showed a similar size and frequency in WT (−13.8 ± 8 pA, 0.16 ± 0.07 Hz; n = 8) and *Eps8*-KO mice (−13 ± 1.1 pA, 0.15 ± 0.06 Hz; n = 10).

(B) Peak amplitude of non-NMDA currents in WT (white bar) and KO (black bar) neurons.

(C) Decay time constants of non-NMDA currents in WT (white bars) and KO (black bars) neurons; the decay time course was fitted with a double exponential function.

(D) Superimposed average NMDA components in cEPSCs of WT (black) and KO (red) neurons normalized for WT amplitude, recorded at +60 mV from the same cells as in (A).

(E) Amplitude of NMDA currents in WT (white bar) and KO neurons (black bar). NMDA amplitude was calculated after 25 ms from EPSC onset (see vertical broken line in [D]).

(F) Weighted decay constant of NMDA current in WT (white bar) and KO (black bar) neurons; the decay time course was fitted with a double exponential function.

reduced the total current in *Eps8*-KO neurons to levels present in wild-type neurons before ethanol exposure (Figure 4J). These findings provide a plausible explanation for the resistance of *Eps8*-KO mice to the acute intoxicating effects of ethanol.

NMDAR-Mediated Signaling Leading to Actin Remodeling Requires Eps8

Converging evidence suggests that the effect of the ablation of *Eps8* on ethanol-dependent phenotypes is due at least in part to altered actin dynamics upon NMDAR activation: (1) Eps8 is physically associated with NMDAR (this paper), (2) the major electrophysiological alteration in *Eps8*-KO CGNs consists of an increase in NMDA currents (this paper), (3) Eps8 regulates actin-cytoskeleton dynamics (Disanza et al., 2004; Scita et al., 1999), (4) NMDAR causes rapid actin remodeling in dendritic spines of hippocampal or cerebellar granule neurons (Fischer et al., 2000; Furuyashiki et al., 2002; Halpain et al., 1998; Shiraishi et al., 2003; Star et al., 2002), and (5) modulation of NMDAR and of NMDAR-originated signals has been widely implicated in neuronal responses to ethanol (Hoffman, 2003). Thus, we directed our attention to the role of Eps8 in NMDAR-induced actin remodeling.

First, we established a suitable model system of CGNs cultured in vitro, which, similar to in vivo CGNs, displayed no significant redundancy of expression of Eps8 family members (Figure 5A). In mature cultured CGNs (>10 days in vitro), Eps8 displayed a distribution similar to that observed in vivo, being localized to the soma and, more importantly, to prominent, F-actin-rich clusters along neurites (Figure 5B). These structures probably represent postsynaptic-like structures, as also witnessed by enrichment of the NMDAR in these structures (Figure 5C). Treatment of cultured CGNs with glutamate or NMDA, but not with AMPA, resulted in almost complete loss of F-actin from the postsynaptic-like structures along the neurites (Figure 5D). Moreover, the specific NMDAR inhibitor MK-801, but not the AMPAR inhibitor CNQX, was able to prevent the effect of glutamate or NMDA (Figure 5D). Finally, the depolymerizing effect of glutamate and NMDA was severely reduced in *Eps8*-KO neurons (Figure 5E), indicating that Eps8 is required for NMDAR-induced actin remodeling.

One of the best characterized NMDAR-dependent pathways, which leads to actin remodeling in neurons, relies on an increase in intracellular calcium, which in turn causes the sequential activation of the phosphatases calcineurin and Slingshot, ultimately controlling cofilin phosphorylation status and activity (Bamburg et al., 1999; Fukazawa et al., 2003; Niwa et al., 2002; Sarmiere and Bamburg, 2004; Wang et al., 2005). Dephosphorylation of cofilin is known to induce its actin depolymerizing and severing activity (Bamburg et al., 1999). In keeping with these observations, treatment of cultured CGNs with glutamate or NMDA led to a significant reduction in the levels of phosphocofilin; however, this effect was severely reduced in *Eps8*-KO CGNs (Figure 5F). Of note, treatment with ethanol did not have any effect on the status of phosphocofilin in either wild-type or *Eps8*-KO CGNs (Figure 5F), a finding that will be subsequently discussed. As a control, we tested the ability of NMDAR to activate ERK in wild-type versus *Eps8*-KO CGNs and found no significant differences (data not shown). This result, together with the shown sustained NMDA currents in *Eps8*-KO CGNs (Figure 4), indicates that the effect of the ablation of *Eps8* on NMDA-induced dephosphorylation of phosphocofilin is not due to a general impairment of the signaling ability of the NMDAR in *Eps8*-KO CGNs. We concluded that Eps8 is required in the NMDAR signaling pathway leading to activation of cofilin and actin-filament turnover.

Functional links among Eps8, Actin, and NMDAR

The above results led to the testable hypothesis that a reduction in actin dynamics might be directly responsible for the increase in NMDA currents in *Eps8*-KO neurons. The electrophysiological alterations detected in *Eps8*-KO neurons could be due directly to the lack of Eps8 function on actin dynamics or to more indirect adaptive changes. Thus, it was important initially to establish whether Eps8 could acutely decrease NMDA currents in *Eps8*-KO neurons. In order to do this, we perfused recombinant Eps8 intracellularly through the patch pipette. Buffer alone had no effect on either the non-NMDA or the NMDA component of cESPCs in *Eps8*-KO neurons (data not shown). Eps8 instead reduced NMDA currents by ~60% in 4 out of 7 *Eps8*-KO neurons tested and increased NMDA currents (~20%) in wild-type neurons (Figures 6A–6C). Interestingly, non-NMDA currents were also slightly reduced in *Eps8*-KO neurons upon Eps8 infusion (Figure 6A).

If increased NMDA currents in *Eps8*-KO neurons are caused by increased actin stability, then they should be sensitive to latrunculin A (LTA)-induced actin depolymerization. We therefore perfused LTA through the patch pipette and recorded cEPSCs. Buffer alone had no effect on cEPSCs (data not shown), and non-NMDA currents were not affected by LTA in either genotype (Figures 6D and 6E). Conversely, the NMDA component of cEPSCs

(G) Inhibition of non-NMDA and NMDA currents by 100 mM (n = 4/genotype) and 400 mM (n = 8/genotype) ethanol in WT (white bars) and KO (black bars) neurons.

(H) Average cEPSCs of NMDA currents recorded at +60 mV before and after ethanol perfusion. Traces were normalized for NMDA amplitude. Vertical scale bar corresponds to 20 pA; horizontal scale bar corresponds to 50 ms. Insets show average cEPSC of non-NMDA currents recorded at −60 mV holding potential before and after ethanol perfusion of the same cell. Vertical scale bar corresponds to 20 pA; horizontal scale bar corresponds to 10 ms.

(I) Time course of NMDA current inhibition by ethanol perfusion (400 mM) in WT (white circles) and KO (black circles) neurons. Values were normalized to the time point prior to the start of ethanol perfusion.

(J) Normalized NMDA charge transfer before and after ethanol perfusion in WT (white bars) and KO (black bars) neurons.

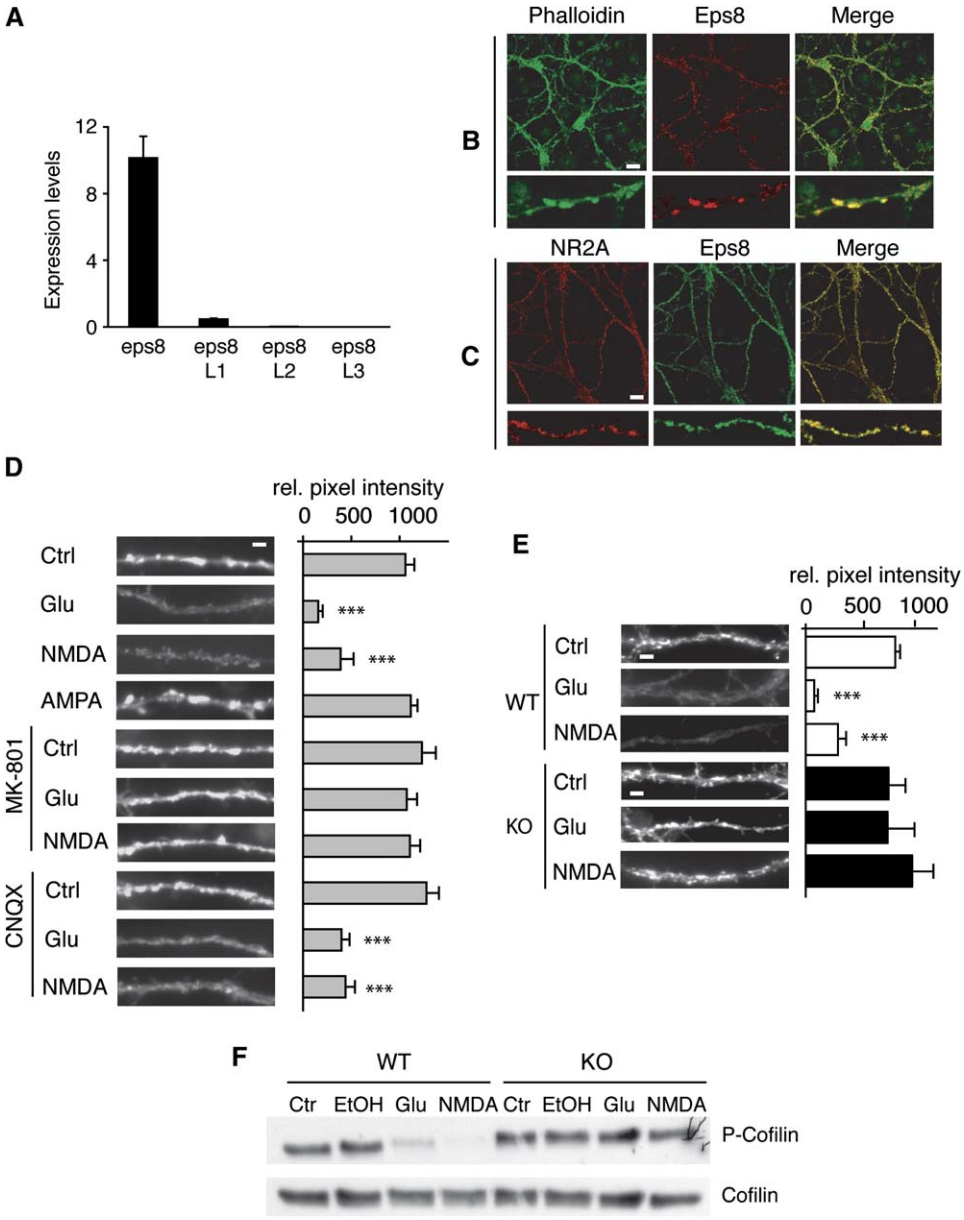

Figure 5. Eps8 in NMDAR-Activated Actin Dynamics

(A) Levels of mRNA (normalized to *18S*) of *Eps8* family members in cultured CGNs.

(B and C) Localization of either Eps8 ([B], red; [C], green) or NR2A ([C], red) and F-actin ([B], phalloidin, green) in cultured CGNs. Bar = 10 μm. The lower panels show a 4.3-fold magnification of the neurites.

(D) CGNs from WT mice were treated with glutamate (Glu, 50 μM, 20 min), NMDA (50 μM, 20 min), or AMPA (100 μM, 20 min) or were mock treated (Ctrl) with or without prior incubation with the NMDAR antagonist MK-801 (0.1 μM, 20 min) or the AMPAR antagonist CNQX (50 μM, 20 min) followed by detection with phalloidin. Bar = 2 μm. In (D) and (E), a quantitative assessment is also shown as relative pixel intensity ± SD (n = 12–27 random neurites per condition).

(E) CGNs from WT or KO mice were treated (as in [D]) with glutamate or NMDA or were mock treated (Ctrl), followed by detection with phalloidin. Bar = 2 μm.

(F) CGNs from WT or KO mice were treated (as in [D]) with glutamate, NMDA, or ethanol (200 mM, 30 min) or were mock treated (Ctr), followed by IB as indicated.

was significantly reduced in *Eps8*-KO but not in wild-type CGNs (Figures 6D–6F). This observation likely reflects an effect of LTA on NMDAR activity that is evidenced only under conditions of altered actin dynamics, such as those induced by Eps8 removal. Whatever the case, increased NMDA currents in *Eps8*-KO neurons can be reversed by

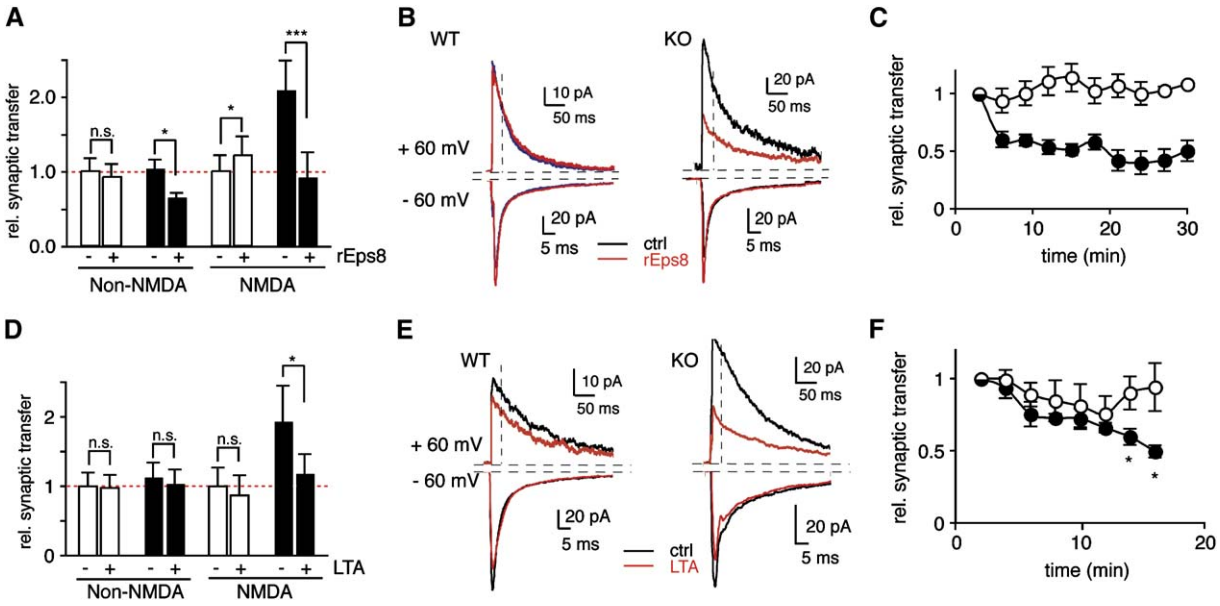

Figure 6. Functional Links among Eps8, Actin, and NMDAR

(A) Effects of recombinant Eps8 (rEps8, 300 nM; − and + indicate before and after perfusion) on normalized non-NMDA peak amplitude (non-NMDA) and NMDA currents (NMDA) of cEPSCs in WT (n = 5, white bars) and KO (n = 4, black bars) neurons. Values in (A) and (D) are normalized to WT before treatment.

(B) Representative traces of the non-NMDA (−60 mV) and NMDA (+60 mV) components of cEPSCs before and 20 min after infusion of recombinant Eps8 in KO neurons.

(C) Time course of normalized synaptic transfer through NMDAR during infusion of recombinant Eps8 in WT (white circles) or KO (black circles) neurons. Values in (C) and (F) are normalized to time point 0.

(D) Effects of LTA (20 μM; − and + indicate before and after perfusion) on normalized non-NMDA peak amplitude (non-NMDA) and NMDA currents (NMDA) of cEPSCs in WT (n = 10, white bars) and KO (n = 13, black bars) neurons.

(E) Representative traces of the non-NMDA (−60 mV) and NMDA (+60 mV) components of cEPSCs before and 15 min after perfusion of LTA.

(F) Time course of the relative synaptic transfer (NMDA current) following LTA perfusion in WT (white circles) or KO (black circles) neurons. Asterisks indicate significance in the comparison between WT and KO. Moreover, in KO neurons, differences were significant with respect to time 0 starting from the 5 min time point (data not shown). In WT neurons, differences with respect to time 0 were not significant (data not shown).

either Eps8 or the actin-depolymerizing drug LTA, in keeping with the hypothesis that these currents are due to increased actin stability.

Ethanol Induces Actin Reorganization in Neurons in an Eps8-Dependent Manner

Ethanol affects actin remodeling in nonneuronal cells (Allansson et al., 2001; Qian et al., 2003), suggesting that it might exert similar effects in neurons. We investigated this possibility in CGNs in vitro. Acute ethanol treatment (200 mM, 30 min) delocalized Eps8, particularly in the postsynaptic-like structures along the neurites, where discrete Eps8 clusters were greatly reduced as a consequence (Figure 7A). This correlated with pronounced loss of F-actin from the same postsynaptic-like structures (Figures 7A and 7B), whereas a synaptic marker, synapsin, did not change upon ethanol treatment (Figures 7A and 7B), arguing against both nonspecific effects of ethanol and major changes in synaptic morphology. Dose- and time-dependence analysis revealed that the effects were already visible after 5 min of ethanol treatment (200 mM) or at doses as low as 50 mM (30 min) (Figures S3A and S3B). The effects of ethanol on F-actin redistribution were reversible within 30 min of ethanol washout (Figure S3C). Application of the NMDAR antagonist MK-801 in conjunction with ethanol did not prevent actin depolymerization, demonstrating that the effects of ethanol were not due to activation of the NMDAR (Figures S3D and S3E).

Eps8-KO neurons displayed resistance to the ethanol-induced remodeling of F-actin (Figures 7C and 7D), and doses as high as 400 mM were needed to observe some F-actin redistribution (Figure 7E). Importantly, the same effects were observed on acute cerebellar slices treated with ethanol ex vivo (Figure 7F). In particular, at 400 mM ethanol—the concentration previously shown to severely inhibit wild-type NMDA currents—almost complete actin depolymerization was observed in wild-type but not *Eps8*-KO slices (Figure 7F).

The lack of Eps8 therefore renders the actin cytoskeleton less sensitive to the remodeling action of ethanol, in line with the demonstrated role of Eps8 in actin dynamics. Part of the action of Eps8 is mediated through its direct interaction with F-actin (Innocenti et al., 2002, 2003; Scita et al., 1999; Croce et al., 2004; Disanza et al., 2004). However, both the in vitro binding activity of Eps8 to F-actin

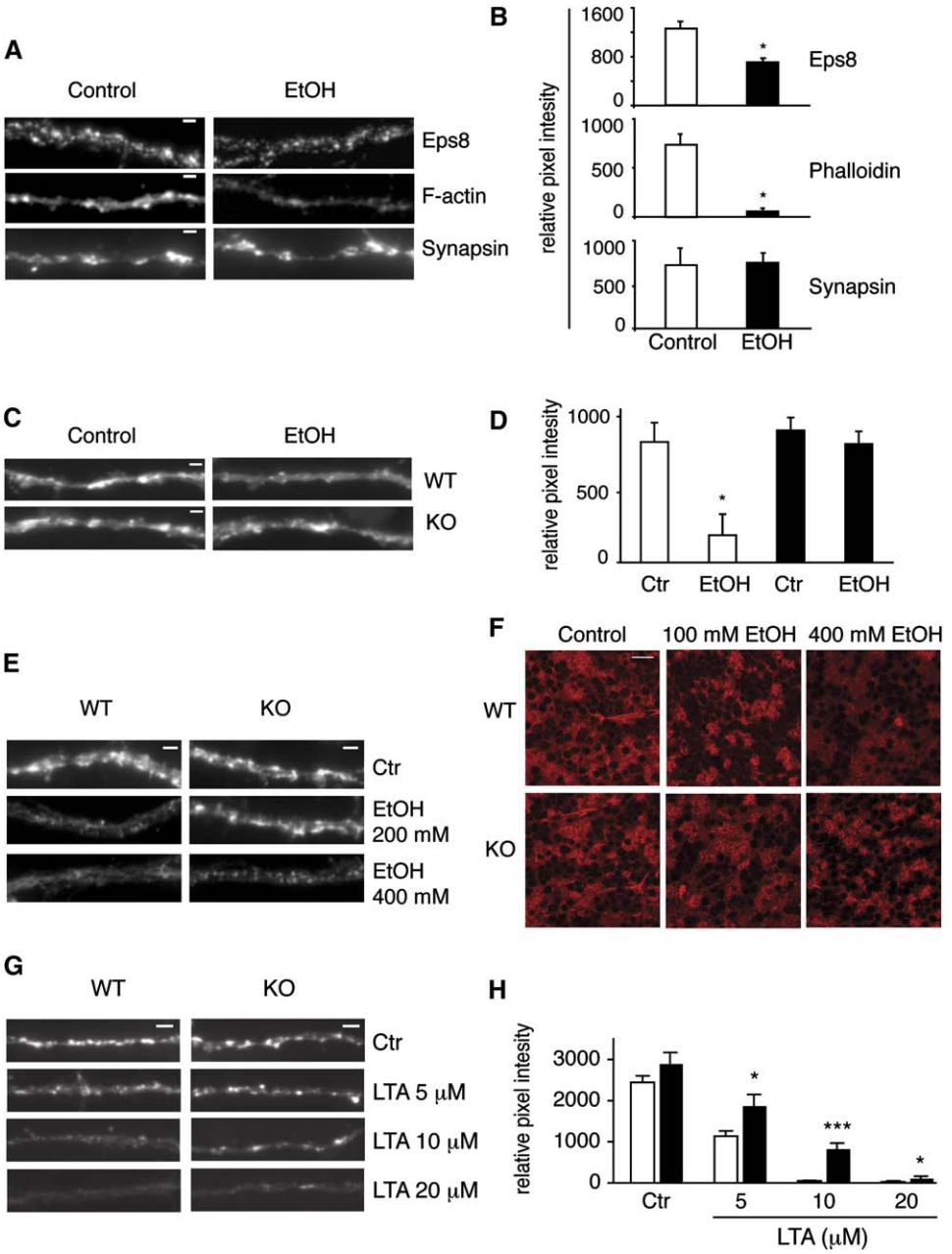

Figure 7. Ethanol Induces Eps8-Dependent Actin Depolymerization in Cultured CGNs

(A) Cultured CGNs from WT mice were treated with ethanol (200 mM, 30 min) or were mock treated (Control), followed by detection by immunofluorescence of Eps8, F-actin, and synapsin. Typical images of neurites are shown. Bar = 2 μm.

(B) Quantitative assessment of the experiment in (A). Data in (B), (D), and (H) are expressed as relative pixel intensity ± SD (n = 10–16 random neurites per condition).

(C) CGNs from WT or KO mice were treated with ethanol (as in [A]) or were mock treated, followed by detection with phalloidin. Bar = 2 μm.

(D) Quantitative assessment of the experiment in (C).

(E and F) Cultured CGNs (E) or cerebellar slices (F) from WT or KO mice were treated with ethanol as indicated (30 min) or were mock treated (Ctr/Control), followed by detection with phalloidin. Bar in (E) = 2 μm; bar in (F) = 25 μm.

(G) Cultured CGNs from WT or KO mice were treated with LTA as indicated (30 min) or were mock treated, followed by detection with phalloidin. Bar = 2 μm.

(H) Quantitative assessment of the experiment in (G).

and the in vitro actin barbed-end-capping activity of Eps8 were unaffected by treatment with ethanol (data not shown). These results argue against a direct effect of ethanol on the Eps8:F-actin interaction and rather suggest, also in light of the results in Figure 5 and Figure 6, that the absence of Eps8 renders the actin cytoskeleton less dynamic and therefore less sensitive to actin-depolymerizing stimuli. To test this possibility, we investigated the effect of LTA on wild-type and *Eps8*-KO neurons. Consistent with the hypothesis, *Eps8*-KO CGNs displayed reduced sensitivity to the actin-depolymerizing effect of LTA (Figures 7G and 7H).

DISCUSSION

Eps8 and Ethanol-Related Behavior

Data in this paper establish that removal of Eps8 in mice causes resistance to the hypnotic and motor-incoordinating effects of ethanol. *Eps8*-KO mice also show increased ethanol consumption. In *Drosophila melanogaster*, the two homologs of Eps8, Arouser and CG8907, regulate acute ethanol sensitivity (D.G and U.H., unpublished data). Thus, Eps8 is part of an evolutionarily conserved circuit that modulates sensitivity to ethanol. We further show that alterations in neuronal actin dynamics underlie the observed phenotype in *Eps8*-KO mice. In an accompanying paper in this issue of *Cell*, Rothenfluh et al. (2006) demonstrate that mutations in RhoGAP18B affect ethanol sensitivity in the fly. Together, these results argue that regulation of the actin cytoskeleton is a key factor in cellular and behavioral responses to ethanol.

Is the Eps8 expression pattern compatible with the observed phenotypes? The expression of Eps8 in the cerebellum is consistent with the resistance of *Eps8*-KO mice to the acute intoxicating effects of ethanol since this phenotype involves cerebellar function (Hanchar et al., 2005; Tabakoff et al., 2003). However, the increased ethanol consumption/preference of *Eps8*-KO mice is less easily conceptualized, as Eps8 is not widely expressed in areas implicated in motivational reward. We cannot exclude that brain areas displaying low/moderate expression of Eps8 are functionally altered in *Eps8*-KO mice. However, we would like to offer an alternative explanation. It is known that chronic exposure to ethanol leads to increased NMDAR activity in mice by diverse mechanisms, e.g., receptor levels, synaptic localization, or posttranslational modifications (Chandler, 2003; Hoffman, 2003). Intriguingly, increased NMDA currents in naive *Eps8*-KO mice mimic this condition, which is reached in wild-type mice after chronic ethanol exposure. Thus, *Eps8*-KO mice might consume more ethanol simply because the rewarding effects of ethanol consumption are not limited (or are less limited) by its intoxicating side effects.

Eps8 in NMDAR Signaling Leading to Actin Remodeling

The major electrophysiological alteration uncovered in *Eps8*-KO CGNs is the increase in NMDA currents, an event that could be directly linked to reduced actin dynamics. There are two implications of these findings. At the phenotypic level, this might account for the resistance of *Eps8*-KO mice to the acute intoxicating effects of ethanol since exposure to ethanol reduces NMDA current in *Eps8*-KO neurons to levels comparable to those of naive (unexposed to ethanol) wild-type neurons. At the molecular level, they implicate Eps8 in the NMDAR pathway. Indeed, the NMDAR signaling pathway leading to activation of cofilin, and hence to actin dynamics, is nonfunctional in *Eps8*-KO neurons.

The NMDAR is connected to the actin cytoskeleton, which links the receptor to molecules involved in its posttranslational modification and in signaling (Salter and Kalia, 2004; Sheng and Kim, 2002). In addition, the NMDAR is thought to activate a negative feedback loop in which an increase in intracellular calcium leads to activation of the phosphatase Slingshot, which, in turn, dephosphorylates cofilin, liberating the actin-remodeling activity of the latter (Huang et al., 2006; Wang et al., 2005). This in turn is thought to downmodulate NMDAR activity (Morishita et al., 2005; Rosenmund and Westbrook, 1993). In *Eps8*-KO CGNs, the decreased ability of NMDAR to induce actin remodeling and the increased NMDA currents at steady state could be due to a defect in this negative regulatory mechanism. The exact role of Eps8 in the NMDAR pathway leading to dephosphorylation of cofilin remains to be established and will be further discussed below.

Eps8 in Ethanol-Induced Actin Remodeling

We show that concentrations of ethanol that are easily reached in the CNS in alcohol-related disorders induce actin remodeling in CGNs, while this effect is attenuated in *Eps8*-KO neurons. Alterations in actin dynamics in dendritic spines are known to accompany and mediate the structural and functional changes associated with synaptic plasticity (Fukazawa et al., 2003; Krucker et al., 2000; Zhou et al., 2004; Zito et al., 2004). Thus, the previously described effect of ethanol on synaptic plasticity (Berry and Matthews, 2004; Blitzer et al., 1990; Krazem et al., 2003) might be mediated in part by alteration of actin-filament turnover.

The resistance of *Eps8*-KO neurons to the actin-remodeling effects of both ethanol and NMDA might suggest common mechanisms. In a simple scenario, ethanol might intercept the NMDAR pathway leading to actin remodeling, mimicking, at some levels, the effects of active NMDAR. However, ethanol does not cause dephosphorylation of cofilin (Figure 5F). Our data are therefore more compatible with the possibility that Eps8 is not directly part of a putative ethanol-signaling pathway. Rather, in *Eps8*-KO mice, the action of ethanol on the actin meshwork might impact on pre-existing reduced actin dynamics, as also supported by the decreased sensitivity of *Eps8*-KO neurons to the actin-depolymerizing effects of LTA.

A Tentative Molecular Model for the Role of Eps8 and Actin Dynamics in Ethanol Responses

We would like to propose a working model that attempts to rationalize the impact of Eps8, and of its regulation of actin dynamics, on ethanol responses and phenotypes. In this model, a first site of action of Eps8 is downstream of NMDAR and upstream of dephosphorylation/activation of cofilin. In the absence of Eps8, this pathway is interrupted, with predicted reduction in actin-filament turnover. A second site of action is unveiled by ethanol and LTA studies in CGNs. In this case, altered dephosphorylation of cofilin is not involved, and the lack of Eps8 seems to cause an increased stability of the actin cytoskeleton. Interestingly, in both cases, the effects of the ablation of *Eps8* seem to converge toward a reduction of actin dynamics.

How does this translate in molecular terms? Eps8 is known to have a dual signaling/structural role in actin dynamics in that it participates in the formation of a multimolecular Rac-GEF complex (Innocenti et al., 2002, 2003; Scita et al., 1999) and is also endowed with actin barbed-end-capping properties (Croce et al., 2004; Disanza et al., 2004). There is reason to believe that the two functions of Eps8 might be differentially involved in the two points of action outlined above. There is emerging evidence that Rac is involved in dephosphorylation/activation of cofilin, possibly through regulation of the phosphatase Slingshot (Nagata-Ohashi et al., 2004). This suggests a simple mechanism through which Eps8 might participate in the NMDAR→cofilin pathway by regulating Rac activity. On the other hand, the actin barbed-end-capping activity of Eps8 might impact actin-cytoskeleton stability, as this function is required for optimal actin dynamics (Pantaloni et al., 2001; Pollard and Borisy, 2003), with consequent increased actin stability in *Eps8*-KO neurons.

In conclusion, our data open new perspectives in ethanol-related disorders in connection with the regulation of stability of the actin cytoskeleton. In this framework, it will be of interest to perform analysis of polymorphisms that might affect Eps8 in human alcoholics.

EXPERIMENTAL PROCEDURES

Animal Experiments

Eps8-KO mice (Scita et al., 1999) were backcrossed for more than ten generations to C57BL/6 mice. For behavioral tests, littermates derived from heterozygous crosses were used; in some experiments, wild-type and KO mice from F2N18 homozygous colonies were also used. Experiments were performed on both male and female mice of 3–5 months of age; since results were comparable, data were pooled, except were indicated. All experiments were performed in accordance with the guidelines established in the IFOM-IEO Campus Principles of Laboratory Animal Care (directive 86/609/EEC).

A modified SHIRPA (Irwin, 1968) was performed according the European Mouse Phenotyping Resource of Standardised Screens (http://www.eumorphia.org/).

For loss of righting reflex, mice were injected intraperitoneally (i.p.) with ethanol (20% in PBS, 4 g/kg body weight) and placed on their back in a U-shaped trough after they lost the ability to right themselves. Sleep time was defined as the time until the mice regained the ability to right themselves on all four paws three times in 30 s. The threshold concentration of ethanol required to induce the loss of righting reflex was determined using the "up and down" method (Dixon, 1965; Wallace et al., 2006).

For rotarod experiments (mouse rotarod treadmill, Ugo Basile; accelerating from 7 to 30 rpm in 300 s), mice were given two trial sessions of five consecutive trials on 2 consecutive days for training (see Figure S1A). On the third day, mice were given one trial session and then received an i.p. injection of PBS (mock treatment) before being tested again after a 30 min recovery time. On the fourth day, PBS was substituted by ethanol (20% in PBS, at the indicated concentrations).

Ethanol-stimulated locomotor activity was assessed by recording the walking activity of the mice every 5 s for 10 min in an open field of 60 × 60 cm. Mice were habituated to the open-field apparatus for two consecutive days. On the third day, mice were injected i.p. with PBS immediately before being placed in the center of the open field. On the fourth day, ethanol (20% in PBS) was substituted for PBS.

For the two-bottle choice test, mice were single housed in cages supplied with two water bottles for one week to allow them to habituate to the test environment. Mice were then offered increasing ethanol concentrations for 8 days each. Tastants were tested sequentially using increasing concentrations of the test solutions each for 4 days. Bottle position was changed daily (every other day in ethanol experiments) to prevent side effects, and liquid and food consumption was registered.

Simple comparisons were made using Student's t test; multiple comparisons were made using two-way repeated-measures ANOVA. Additional details for the procedures of the behavioral experiments can be found in Supplemental Experimental Procedures.

Standard histological and immuno-EM procedures are described in Supplemental Experimental Procedures.

Studies with Cerebellar Granule Neurons

CGNs from cerebella from P6/P7 mice were prepared using the Papain Dissociation System (Worthington; see also Supplemental Experimental Procedures).

For immunofluorescence, CGNs were fixed in 4% paraformaldehyde for 10 min, permeabilized with 0.05% Triton X-100 in TBS plus 1% BSA, and then incubated with primary Ab at 4°C overnight. Appropriate secondary antibodies conjugated to Cy3 or FITC (Jackson) were applied subsequently. F-actin was detected with TRITC- or FITC-conjugated phalloidin (Sigma). Analysis was with a 40× objective or 60× oil-immersion objective plus a 1.6× zoom affixed to a Leica DMR microscope. Digital images were collected using a Hamamatsu C5985 B/W CCD camera and acquired with the Hamamatsu C5985/C5810 plug-in using identical settings for each data set.

For quantitative analyses, neurons were randomly selected from areas of the coverslip where cultures were less dense, and 10–30 neurites per condition (corresponding to ~400 μm–1.2 mm total neurite length) were analyzed using ImageJ (http://rsb.info.nih.gov/ij/) (see also Supplemental Experimental Procedures).

Biochemical Studies

Synaptosomal and PSD fractions were prepared as described (Carlin et al., 1980). Anti-synaptophysin (ListarFISH) and anti-PSD-95 (Affinity Bioreagent) were used to assess the purity/enrichment of the fractions.

For coimmunoprecipitation, adult cerebella were lysed in RIPA buffer containing protease and phosphatase inhibitors. Antibodies used for immunoprecipitation were obtained from Santa Cruz (NR1, NR2A, NR2B, and NR2C) or Upstate (GluR1). A list of all antibodies used in this study is in Supplemental Experimental Procedures.

Electrophysiological Recordings

Whole-cell patch-clamp recordings were performed from granule cells in the internal granular layer of acute cerebellar slices obtained from 18- to 24-day-old wild-type and *Eps8*-KO mice as previously described (D'Angelo et al., 1999; Rossi et al., 2002). A detailed description is in Supplemental Experimental Procedures.

Supplemental Data

Supplemental Data include Supplemental Experimental Procedures, Supplemental References, three figures, and six tables and can be found with this article online at http://www.cell.com/cgi/content/full/127/1/213/DC1/.

ACKNOWLEDGMENTS

We thank P. Transidico and M. Garrè for technical assistance. This work was supported by grants from the Associazione Italiana per la Ricerca sul Cancro, Ministero della Salute, MIUR, and Fondazione Monzino to P.P.D.F.; NIH grants AA13105 and AA10035 to U.H.; and grants from the European Community (VI Framework) to P.P.D.F. and E.D.

Received: March 10, 2006
Revised: July 30, 2006
Accepted: September 8, 2006
Published: October 5, 2006

REFERENCES

Allansson, L., Khatibi, S., Olsson, T., and Hansson, E. (2001). Acute ethanol exposure induces [Ca2+]i transients, cell swelling and transformation of actin cytoskeleton in astroglial primary cultures. J. Neurochem. *76*, 472–479.

Bachmanov, A.A., Reed, D.R., Tordoff, M.G., Price, R.A., and Beauchamp, G.K. (1996). Intake of ethanol, sodium chloride, sucrose, citric acid, and quinine hydrochloride solutions by mice: a genetic analysis. Behav. Genet. *26*, 563–573.

Bamburg, J.R., McGough, A., and Ono, S. (1999). Putting a new twist on actin: ADF/cofilins modulate actin dynamics. Trends Cell Biol. *9*, 364–370.

Belknap, J.K., Crabbe, J.C., and Young, E.R. (1993). Voluntary consumption of ethanol in 15 inbred mouse strains. Psychopharmacology (Berl.) *112*, 503–510.

Berry, R.B., and Matthews, D.B. (2004). Acute ethanol administration selectively impairs spatial memory in C57BL/6J mice. Alcohol *32*, 9–18.

Blitzer, R.D., Gil, O., and Landau, E.M. (1990). Long-term potentiation in rat hippocampus is inhibited by low concentrations of ethanol. Brain Res. *537*, 203–208.

Bowers, B.J. (2000). Applications of transgenic and knockout mice in alcohol research. Alcohol Res. Health *24*, 175–184.

Capani, F., Ellisman, M.H., and Martone, M.E. (2001). Filamentous actin is concentrated in specific subpopulations of neuronal and glial structures in rat central nervous system. Brain Res. *923*, 1–11.

Carlin, R.K., Grab, D.J., Cohen, R.S., and Siekevitz, P. (1980). Isolation and characterization of postsynaptic densities from various brain regions: enrichment of different types of postsynaptic densities. J. Cell Biol. *86*, 831–845.

Carpenter-Hyland, E.P., Woodward, J.J., and Chandler, L.J. (2004). Chronic ethanol induces synaptic but not extrasynaptic targeting of NMDA receptors. J. Neurosci. *24*, 7859–7868.

Chandler, L.J. (2003). Ethanol and brain plasticity: receptors and molecular networks of the postsynaptic density as targets of ethanol. Pharmacol. Ther. *99*, 311–326.

Crabbe, J.C., Phillips, T.J., Feller, D.J., Hen, R., Wenger, C.D., Lessov, C.N., and Schafer, G.L. (1996). Elevated alcohol consumption in null mutant mice lacking 5-HT1B serotonin receptors. Nat. Genet. *14*, 98–101.

Crabbe, J.C., Metten, P., Cameron, A.J., and Wahlsten, D. (2005). An analysis of the genetics of alcohol intoxication in inbred mice. Neurosci. Biobehav. Rev. *28*, 785–802.

Croce, A., Cassata, G., Disanza, A., Gagliani, M.C., Tacchetti, C., Malabarba, M.G., Carlier, M.F., Scita, G., Baumeister, R., and Di Fiore, P.P. (2004). A novel actin barbed-end-capping activity in EPS-8 regulates apical morphogenesis in intestinal cells of Caenorhabditis elegans. Nat. Cell Biol. *6*, 1173–1179.

D'Angelo, E., Rossi, P., Armano, S., and Taglietti, V. (1999). Evidence for NMDA and mGlu receptor-dependent long-term potentiation of mossy fiber-granule cell transmission in rat cerebellum. J. Neurophysiol. *81*, 277–287.

Dillon, C., and Goda, Y. (2005). The actin cytoskeleton: integrating form and function at the synapse. Annu. Rev. Neurosci. *28*, 25–55.

Disanza, A., Carlier, M.F., Stradal, T.E., Didry, D., Frittoli, E., Confalonieri, S., Croce, A., Wehland, J., Di Fiore, P.P., and Scita, G. (2004). Eps8 controls actin-based motility by capping the barbed ends of actin filaments. Nat. Cell Biol. *6*, 1180–1188.

Dixon, W.J. (1965). The Up-and-Down method for small samples. JAMA *60*, 967–978.

Fischer, M., Kaech, S., Wagner, U., Brinkhaus, H., and Matus, A. (2000). Glutamate receptors regulate actin-based plasticity in dendritic spines. Nat. Neurosci. *3*, 887–894.

Fukazawa, Y., Saitoh, Y., Ozawa, F., Ohta, Y., Mizuno, K., and Inokuchi, K. (2003). Hippocampal LTP is accompanied by enhanced F-actin content within the dendritic spine that is essential for late LTP maintenance in vivo. Neuron *38*, 447–460.

Furuyashiki, T., Arakawa, Y., Takemoto-Kimura, S., Bito, H., and Narumiya, S. (2002). Multiple spatiotemporal modes of actin reorganization by NMDA receptors and voltage-gated Ca2+ channels. Proc. Natl. Acad. Sci. USA *99*, 14458–14463.

Halpain, S., Hipolito, A., and Saffer, L. (1998). Regulation of F-actin stability in dendritic spines by glutamate receptors and calcineurin. J. Neurosci. *18*, 9835–9844.

Hanchar, H.J., Dodson, P.D., Olsen, R.W., Otis, T.S., and Wallner, M. (2005). Alcohol-induced motor impairment caused by increased extrasynaptic GABA(A) receptor activity. Nat. Neurosci. *8*, 339–345.

Hoffman, P.L. (2003). NMDA receptors in alcoholism. Int. Rev. Neurobiol. *56*, 35–82.

Hoffman, P.L., Rabe, C.S., Moses, F., and Tabakoff, B. (1989). N-methyl-D-aspartate receptors and ethanol: inhibition of calcium flux and cyclic GMP production. J. Neurochem. *52*, 1937–1940.

Honse, Y., Ren, H., Lipsky, R.H., and Peoples, R.W. (2004). Sites in the fourth membrane-associated domain regulate alcohol sensitivity of the NMDA receptor. Neuropharmacology *46*, 647–654.

Huang, T.Y., Dermardirossian, C., and Bokoch, G.M. (2006). Cofilin phosphatases and regulation of actin dynamics. Curr. Opin. Cell Biol. *18*, 26–31.

Husi, H., Ward, M.A., Choudhary, J.S., Blackstock, W.P., and Grant, S.G. (2000). Proteomic analysis of NMDA receptor-adhesion protein signaling complexes. Nat. Neurosci. *3*, 661–669.

Innocenti, M., Tenca, P., Frittoli, E., Faretta, M., Tocchetti, A., Di Fiore, P.P., and Scita, G. (2002). Mechanisms through which Sos-1 coordinates the activation of Ras and Rac. J. Cell Biol. *156*, 125–136.

Innocenti, M., Frittoli, E., Ponzanelli, I., Falck, J.R., Brachmann, S.M., Di Fiore, P.P., and Scita, G. (2003). Phosphoinositide 3-kinase activates Rac by entering in a complex with Eps8, Abi1, and Sos-1. J. Cell Biol. *160*, 17–23.

Irwin, S. (1968). Comprehensive observational assessment: Ia. A systematic, quantitative procedure for assessing the behavioral and physiologic state of the mouse. Psychopharmacologia *13*, 222–257.

Kampov-Polevoy, A.B., Garbutt, J.C., and Janowsky, D.S. (1999). Association between preference for sweets and excessive alcohol intake: a review of animal and human studies. Alcohol Alcohol. *34*, 386–395.

Krazem, A., Marighetto, A., Higueret, P., and Jaffard, R. (2003). Age-dependent effects of moderate chronic ethanol administration on

different forms of memory expression in mice. Behav. Brain Res. *147*, 17–29.

Krucker, T., Siggins, G.R., and Halpain, S. (2000). Dynamic actin filaments are required for stable long-term potentiation (LTP) in area CA1 of the hippocampus. Proc. Natl. Acad. Sci. USA *97*, 6856–6861.

Li, T.K., Lumeng, L., and Doolittle, D.P. (1993). Selective breeding for alcohol preference and associated responses. Behav. Genet. *23*, 163–170.

Lovinger, D.M., White, G., and Weight, F.F. (1989). Ethanol inhibits NMDA-activated ion current in hippocampal neurons. Science *243*, 1721–1724.

Morishita, W., Marie, H., and Malenka, R.C. (2005). Distinct triggering and expression mechanisms underlie LTD of AMPA and NMDA synaptic responses. Nat. Neurosci. *8*, 1043–1050.

Nagata-Ohashi, K., Ohta, Y., Goto, K., Chiba, S., Mori, R., Nishita, M., Ohashi, K., Kousaka, K., Iwamatsu, A., Niwa, R., et al. (2004). A pathway of neuregulin-induced activation of cofilin-phosphatase Slingshot and cofilin in lamellipodia. J. Cell Biol. *165*, 465–471.

Niwa, R., Nagata-Ohashi, K., Takeichi, M., Mizuno, K., and Uemura, T. (2002). Control of actin reorganization by Slingshot, a family of phosphatases that dephosphorylate ADF/cofilin. Cell *108*, 233–246.

Offenhäuser, N., Borgonovo, A., Disanza, A., Romano, P., Ponzanelli, I., Iannolo, G., Di Fiore, P.P., and Scita, G. (2004). The eps8 family of proteins links growth factor stimulation to actin reorganization generating functional redundancy in the Ras/Rac pathway. Mol. Biol. Cell *15*, 91–98.

Pantaloni, D., Le Clainche, C., and Carlier, M.F. (2001). Mechanism of actin-based motility. Science *292*, 1502–1506.

Peoples, R.W., and Stewart, R.R. (2000). Alcohols inhibit N-methyl-D-aspartate receptors via a site exposed to the extracellular environment. Neuropharmacology *39*, 1681–1691.

Pollard, T.D., and Borisy, G.G. (2003). Cellular motility driven by assembly and disassembly of actin filaments. Cell *112*, 453–465.

Qian, Y., Luo, J., Leonard, S.S., Harris, G.K., Millecchia, L., Flynn, D.C., and Shi, X. (2003). Hydrogen peroxide formation and actin filament reorganization by Cdc42 are essential for ethanol-induced in vitro angiogenesis. J. Biol. Chem. *278*, 16189–16197.

Roberto, M., Schweitzer, P., Madamba, S.G., Stouffer, D.G., Parsons, L.H., and Siggins, G.R. (2004). Acute and chronic ethanol alter glutamatergic transmission in rat central amygdala: an in vitro and in vivo analysis. J. Neurosci. *24*, 1594–1603.

Ron, D. (2004). Signaling cascades regulating NMDA receptor sensitivity to ethanol. Neuroscientist *10*, 325–336.

Rosenmund, C., and Westbrook, G.L. (1993). Calcium-induced actin depolymerization reduces NMDA channel activity. Neuron *10*, 805–814.

Rossi, P., Sola, E., Taglietti, V., Borchardt, T., Steigerwald, F., Utvik, J.K., Ottersen, O.P., Kohr, G., and D'Angelo, E. (2002). NMDA receptor 2 (NR2) C-terminal control of NR open probability regulates synaptic transmission and plasticity at a cerebellar synapse. J. Neurosci. *22*, 9687–9697.

Rothenfluh, A., Threlkeld, R.J., Bainton, R.J., Tsai, L.T.-Y., Lasek, A.W., and Heberlein, U. (2006). Distinct behavioral responses to ethanol are regulated by alternate RhoGAP18B isoforms. Cell *127*, this issue, 199–211.

Rustay, N.R., Wahlsten, D., and Crabbe, J.C. (2003). Assessment of genetic susceptibility to ethanol intoxication in mice. Proc. Natl. Acad. Sci. USA *100*, 2917–2922.

Salter, M.W., and Kalia, L.V. (2004). Src kinases: a hub for NMDA receptor regulation. Nat. Rev. Neurosci. *5*, 317–328.

Sarmiere, P.D., and Bamburg, J.R. (2004). Regulation of the neuronal actin cytoskeleton by ADF/cofilin. J. Neurobiol. *58*, 103–117.

Schuckit, M.A., and Smith, T.L. (2000). The relationships of a family history of alcohol dependence, a low level of response to alcohol and six domains of life functioning to the development of alcohol use disorders. J. Stud. Alcohol *61*, 827–835.

Scita, G., Nordstrom, J., Carbone, R., Tenca, P., Giardina, G., Gutkind, S., Bjarnegard, M., Betsholtz, C., and Di Fiore, P.P. (1999). EPS8 and E3B1 transduce signals from Ras to Rac. Nature *401*, 290–293.

Sheng, M., and Kim, M.J. (2002). Postsynaptic signaling and plasticity mechanisms. Science *298*, 776–780.

Shiraishi, Y., Mizutani, A., Yuasa, S., Mikoshiba, K., and Furuichi, T. (2003). Glutamate-induced declustering of post-synaptic adaptor protein Cupidin (Homer 2/vesl-2) in cultured cerebellar granule cells. J. Neurochem. *87*, 364–376.

Star, E.N., Kwiatkowski, D.J., and Murthy, V.N. (2002). Rapid turnover of actin in dendritic spines and its regulation by activity. Nat. Neurosci. *5*, 239–246.

Tabakoff, B., Bhave, S.V., and Hoffman, P.L. (2003). Selective breeding, quantitative trait locus analysis, and gene arrays identify candidate genes for complex drug-related behaviors. J. Neurosci. *23*, 4491–4498.

Wallace, M.J., Newton, P.M., Oyasu, M., McMahon, T., Chou, W.H., Connolly, J., and Messing, R.O. (2006). Acute Functional Tolerance to Ethanol Mediated by Protein Kinase C varepsilon. Neuropsychopharmacology. Published online March 15, 2006. 10.1038/sj.npp.1301059.

Wang, Y., Shibasaki, F., and Mizuno, K. (2005). Calcium signal-induced cofilin dephosphorylation is mediated by Slingshot via calcineurin. J. Biol. Chem. *280*, 12683–12689.

Woodward, J.J. (2000). Ethanol and NMDA receptor signaling. Crit. Rev. Neurobiol. *14*, 69–89.

Wyszynski, M., Lin, J., Rao, A., Nigh, E., Beggs, A.H., Craig, A.M., and Sheng, M. (1997). Competitive binding of alpha-actinin and calmodulin to the NMDA receptor. Nature *385*, 439–442.

Yamada, K., Fukaya, M., Shimizu, H., Sakimura, K., and Watanabe, M. (2001). NMDA receptor subunits GluRepsilon1, GluRepsilon3 and GluRzeta1 are enriched at the mossy fibre-granule cell synapse in the adult mouse cerebellum. Eur. J. Neurosci. *13*, 2025–2036.

Zhou, Q., Homma, K.J., and Poo, M.M. (2004). Shrinkage of dendritic spines associated with long-term depression of hippocampal synapses. Neuron *44*, 749–757.

Zito, K., Knott, G., Shepherd, G.M., Shenolikar, S., and Svoboda, K. (2004). Induction of spine growth and synapse formation by regulation of the spine actin cytoskeleton. Neuron *44*, 321–334.